Conference materials
UDC 547.458.1:[539.25+539.26]
DOI: https://doi.org/10.18721/JPM.153.321

Comparative analysis of nanosized structures in thin hydrogel plates of chitosan L- and D-ascorbate–hydrochloride

A. B. Shipovskaya [1]✉, N. O. Gegel [1], T. S. Babicheva [1]

[1] Saratov State Univercity, Saratov, Russia

✉ Shipovskayaab@yandex.ru

Abstract. Transmission electron microscopy and small-angle X-ray scattering were used to explore the supramolecular structure of thin hydrogel plates of chitosan L- and D-ascorbate–hydrochloride. The objects reveal dendritic formations and structures of fractal dimension at the macrolevel and nanolevel of organization of polymeric substance, respectively. A comparative analysis of the morphology and average size of phase inhomogeneities and their bulk distribution in the material depending on the ascorbic acid isomer (L or D) was carried out.

Keywords: L- (D-) chitosan ascorbate hydrochloride, hydrogel plates, transmission electron microscopy, small-angle X-ray scattering

Funding: The work was carried out within the framework of the grant of the Russian Science Foundation No. 22-23-00320. https://rscf.ru/project/22-23-00320/.

Citation: Shipovskaya A. B., Gegel N. O., Babicheva T. S., Comparative analysis of nanosized structures in thin hydrogel plates of chitosan L- and D-ascorbate–hydrochloride. St. Petersburg State Polytechnical University Journal. Physics and Mathematics, 15 (3.3) (2022) 111–117. DOI: https://doi.org/10.18721/JPM.153.321

Материалы конференции
УДК 547.458.1:[539.25+539.26]
DOI: https://doi.org/10.18721/JPM.153.321

Сравнительный анализ наноразмерных структур в тонких гидрогелевых пластинах L- и D-аскорбата-гидрохлорида хитозана

А. Б. Шиповская [1]✉, Н. О. Гегель [1], Т. С. Бабичева [1]

[1] Саратовский национальный исследовательский государственный университет имени Н. Г. Чернышевского, Саратов, Россия

✉ Shipovskayaab@yandex.ru

Аннотация. Методами просвечивающей электронной микроскопии и малоуглового рентгеновского рассеяния изучена надмолекулярная структура тонких гидрогелевых пластин L- и D-аскорбата-гидрохлорида хитозана. На макроуровне организации полимерного вещества обнаруживаются дендритные образования, наноуровне – структуры фрактальной размерности. Проведен сравнительный анализ морфологии и среднего размера фазовых неоднородностей и их объемного распределения в материале в зависимости от изомера аскорбиновой кислоты (L или D).

Ключевые слова: L- (D-) аскорбат-гидрохлорида хитозана, гидрогелевые пластины, просвечивающая электронная микроскопия, малоугловое рассеяние рентгеновских лучей

Финансирование: Работа выполнена в рамках гранта Российского научного фонда № 22-23-00320. https://rscf.ru/project/22-23-00320/.

Ссылка при цитировании: Шиповская А. Б., Гегель Н. О., Бабичева Т. С., Сравнительный анализ наноразмерных структур в тонких гидрогелевых пластинах

L- и D-аскорбата-гидрохлорида хитозана // Научно-технические ведомости СПбГПУ. Физико-математические науки. 2022. Т. 15. № 3.3. С. 111–117. DOI: https://doi.org/10.18721/JPM.153.321

Introduction

In recent years, along with the dynamically developing biomedical lead of using the aminopolysaccharide chitosan, there is great interest in obtaining thin-film nanocomposite materials based thereon for solving applied problems of optoelectronics and optosensorics, in particular, for designing highly sensitive and highly selective planar waveguides, detectors, and optical sensors for analytical applications [1–6]. Such optical materials are used to diagnose biological macromolecules (DNA, proteins), cells and genetic markers [1], to monitor small organic molecules [2, 3], to analyze trace amounts of heavy metal ions [4], to design sensors for gaseous hydrogen sulfide [5] and integrated optical humidity sensors [6]. The choice of chitosan for creating an optically sensitive layer is determined not only by the formation of thin film substrates, encapsulation and stabilization of various microobjects and nanoparticles therein, but also by the possibility of making hydrogel coatings with nanosized supramolecular ordering. In addition, this aminopolysaccharide is soluble in a slightly acidic aqueous medium, including aqueous solutions of biologically active carboxylic acids, and is obtained from annually renewable natural resources. In this connection, the use of chitosan as an alternative to synthetic and even inorganic materials in optics contributes to the development of environmentally friendly technologies.

Transmission electron microscopy (TEM) is widely used to assess the geometric characteristics and topology of the nanosized structure of chitosan-containing hydrogel materials; while small-angle X-ray scattering (SAXS) is employed for structural diagnostics of condensed phased of polymeric substance at a nanometer scale, obtaining information of the molecular order of a polydisperse system, evaluation of the size of scattering nanosized inhomogeneities [7–11]. The TEM method provides for direct visualization of nanostructures in thin objects, but characterizes their surface morphology only within a limited area of the test sample. The SAXS method significantly complements and extends TEM, since it allows analyzing the nature and fractal dimension of scattering objects, as well as to obtain averaged characteristics of scattering aggregates and their size distribution.

Previously, the authors of this paper prepared hydrogel thin-film plates based on chitosan L-(D-)ascorbate by template sol-gel synthesis, considered the rheokinetics of the process, and estimated the deformation-strength characteristics of the material [12–14]. It was found that the gelation time during the formation of such plates decreases with a decrease in the polymer concentration and an increase in the reaction temperature. The load-elongation curves obtained for all samples are typical for soft elastic materials with macroscopic plasticity. Chitosan D-ascorbate retarded gelation and raised the strength-elastic properties of sol-gel plates in comparison with chitosan L-ascorbate. In addition, chitosan L- and D-ascorbates differed in the condensed macrophase morphology, as well as in the conformation and chirooptic characteristics of macromolecules: the maximum wavelength of the dichroic band and the values of its specific ellipticity, the sign of specific optical rotation, and the type of dispersion curves. It seems that the differences found in the chiral organization of the spatial structure of our hydrogel plates based on chitosan L-(D-)ascorbate, as well as the differences (described in Ref. [15]) in the reactivity of L- and D-ascorbic acid with with respect to chitosan and in the parameters of the monoclinic cell of anhydrous crystals of chitosan L- and D-ascorbate may also have a significant effect on the supramolecular structure of the chitosan-containing hydrogel system at the nanoscale level of its organization.

The purpose of this work was to explore the structure and supramolecular ordering of thin hydrogel sheets of chitosan L- and D-ascorbate-hydrochloride using TEM and SAXS methods.

Materials and Methods

The following reagents were used: chitosan hydrochloride (CS·HCl) with a viscosity average molecular weight of 38 kDa and a degree of deceleration DD = 80 mol.% (Bioprogress Ltd., RF); L-ascorbic acid (L-AscA, ZAO FP Meligen, RF), D-isoascorbic acid (D-AscA, ZAO Khimreaktiv, RF); polyvinyl alcohol (PVA, structurant) with a weight average molecular weight of 89–98 kDa (Sigma Aldrich, USA); a solution of silicon tetraglycerolate in glycerol ($Si(C_3H_7O_3)_4 \cdot 3C_3H_8O_3$, a gelling agent) with a concentration of 58.7 wt.%, obtained in the laboratory of organic materials, Institute of Organic Synthesis named after I. Ya. Postovsky, Ural Branch of the Russian Academy of Sciences (RF) according to the method from Ref. [16]; Milli-Q distilled water. All reagents were chemically pure and were used without further purification.

Aqueous solutions CS·HCl in L-AscA and D-AscA of a concentration of 4 wt.% were prepared in a $-NH_2$:AscA equimolar ratio and used in our experiments. To prepare solutions a sample of CS·HCl powder was suspended in the calculated amount of water on a magnetic stirrer, followed by addition of an air-dry L-(D-)AscA powder. The system was left at 20 ± 2 °C for one day until complete dissolution. Aqueous PVA solutions of a concentration of 10 wt.% were prepared by suspending a sample of polymer powder in the calculated amount of water on a magnetic stirrer for 5 min, followed by 850 W microwave treatment in a laboratory microwave system Mars-5 (CEM Corporation, USA) during 30–50 s.

TEM images were obtained on a transmission electron microscope A Libra 120 (Carl Zeiss, Germany) at 120 kV. Hydrogel plates were fixed with glutaraldehyde for 12 h, dehydrated in increasing concentrations of ethyl alcohol (30, 50, 70, 80, and 96%), absolute acetone and propylene oxide, then embedded with EPON-812© epoxy resin and kept at 37, 45 and 57 °C for 24 h at each temperature. Ultrathin sections were obtained on an LKB-III microtome (Sweden) and applied to a formvar-coated copper grid.

SAXS measurements were carried out on a Hecus S3-MICRO small-angle diffractometer (Austria) with a Kratky collimation system, Cu Kα radiation at a voltage of 50 kV and a current of 1 mA, using a 1D-PSD 50 M detector with a resolution of 1024 pixels. The distance from the quartz cell with the hydrogel plate to the detector was 281 mm. The measurements were carried out in vacuum at 295 K, exposure time 1,000 sec. Scattering intensity $I(q)$ was recorded in the range of the scattering wave vector modulus $q = 0.01–0.65$ Å^{-1}, where $q = 4\pi \sin\theta/\lambda$, 2θ being the scattering angle (deg), λ the radiation wavelength (1.542 Å). Scattering curves were normalized using Lupolen software. The structural parameter n, which characterizes the morphology of scattering inhomogeneities, was calculated from the slope of the straight sections of the scattering curve in the ($\ln I$; q) coordinates, the average radius of gyration R_n of scattering inhomogeneities (in our case, having the physical meaning of the average size of scattering domains) was calculated from the dependence in Guinier coordinates ($\ln I$; q^2) [11, 17]. The size distribution function of inhomogeneities $D_V = f(R)$, where R is the average size of scattering domains, was calculated using the GNOM software [18].

Results and Discussion

Fig. 1 shows the TEM images of ultrathin sections of hydrogel plates of chitosan L- and D-ascorbate-hydrochloride, hereinafter referred to as CS·HCl·L-AscA and CS·HCl·D-AscA. Analysis of these TEM photos shows the presence of two phases in the structure of the samples, namely: an optically "inert" denser phase of the structurant and gelation agent and an optically less dense condensed phase of chitosan ascorbate, represented by supramolecular aggregates of a dendritic-like type. The dendritic structures have a center and relatively extended branches up to ~3–5 μm in length. However, the structure and morphology of dendrites, the size and number of side branches depend on the AscA isomer used to obtain the hydrogel plates (Table 1).

For example, a highly branched dendritic structure with dense symmetrical filamentous branches was observed for the CS·HCl·L-AscA samples. The width of the main and lateral branches was ~0.3–0.4 μm and ~0.2–0.3 μm, respectively. The angle between the axes of the main branches varied in a range of ~60–70°. The geometry and topological characteristics of the dendritic structure of the CS·HCl·D-AscA sample differed significantly. First of all, the supramolecular formations were less branched and less regular. Almost no formation of symmetrical branches was observed. The width of the main and side branches, as well as the angle between the axes of the main branches, increased and amounted to ~0.9–1.2 μm, ~0.5–0.8 μm, and ~80–90°, respectively.

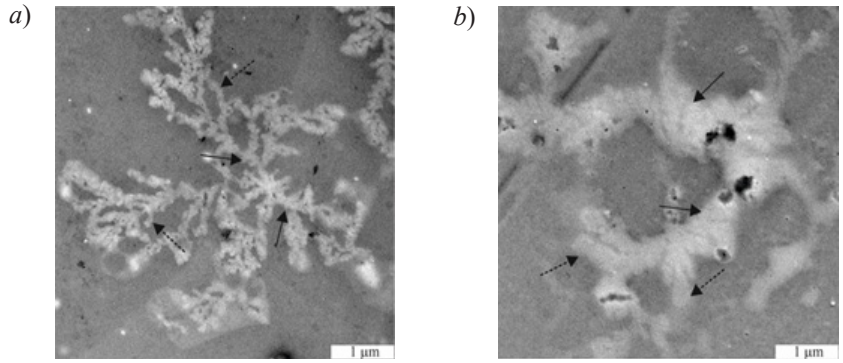

Fig. 1. TEM images of ultrathin sections of our hydrogel plates based on CS·HCl·L-AscA (*a*) and CS·HCl·D-AscA (*b*); smooth arrows mark the main branches of dendritic structures, while dotted arrows mark lateral branches

Table 1

Structural and dimensional characteristics of the supramolecular ordering of hydrogel plates of chitosan L- and D-ascorbate-hydrochloride from TEM and SAXS data

Parameter CS·HCl·L-AscA		Sample	
		CS·HCl·*D*-AscA	CS·HCl·*D*-AscA
TEM			
Branch index		5 ± 1	3 ± 1
Main branch length (μm)		3.5 ± 0.5	4.5 ± 0.5
Main branches width (μm)		0.35 ± 0.05	1.05 ± 0.15
Side branch width (μm)		0.25 ± 0.05	0.65 ± 0.15
Angle between the axes of the main branches (deg)		65 ± 5	80 ± 5
SAXS			
Power decay exponent in the dependence $\ln I(q) = f(q)$, n	I	2.4	2.1
	II	1.8	1.7
Fractal dimension		2.4	2.1
Average radius of gyration of scattering inhomogeneities, R_n (Å)		15–170	25–190
Average size of the dominant fraction of scattering domains, R (Å)		15–85	25–70
Volume fraction of the predominant fraction of scattering domains, $D_V \cdot 10$		3.8	6.0

Besides, the dendrite morphostructure was looser, and the number of side branches was significantly less compared to the sample obtained using the AscA L-isomer.

The intensity curves of small-angle X-ray scattering by CS·HCl·L-AscA and CS·HCl·D-AscA hydrogel plates in semilogarithmic coordinates smoothly decreased with the scattering wave vector modulus and had no Bragg peaks, which indicated scattering by loose-packed inhomogeneity domains and amorphous structure of the samples (Fig. 2). The scattering indicatrices $\ln I(q) = f(q)$ can be divided into two rectilinear sections (I and II), differing in the nature of the angular dependence of the radiation intensity $I(q) \sim q^{-n}$. The first and second corresponded to the scattering coordinate range $q < 0.02$ Å^{-1} and $q \sim 0.02 - 0.11$ Å^{-1}, respectively. $q \sim 0.02$ Å^{-1} can be considered as the crossover point. The decay exponent at low values q, equal to $n = 2.4$ and 2.1 for CS·HCl·L-AscA and CS·HCl·D-AscA, respectively (Table 1), indicates the presence of

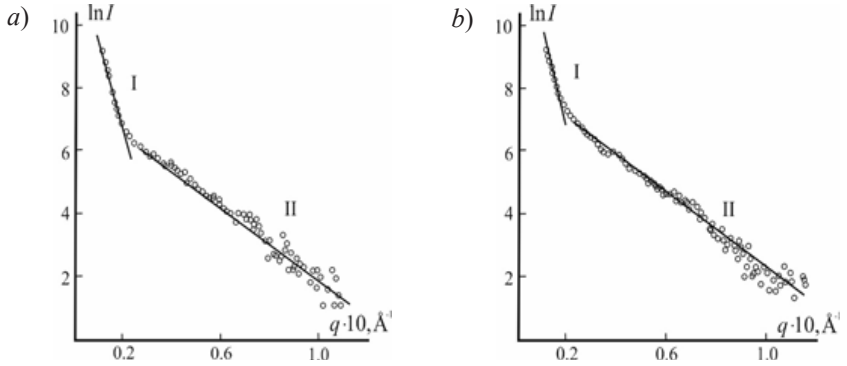

Fig. 2. Curves of small-angle X-ray scattering for hydrogel plates based on CS·HCl·L-AscA (*a*) and CS·HCl·D-AscA (*b*)

scattering bulk domains with a fractal structure in the hydrogel spatial network (bulk fractals) [8, 11]. In the range of higher q values, the slope of the SAXS curve for the same samples is $n = 1.8$ and $n = 1.7$, respectively. This means that polymer coils in scattering inhomogeneities have the conformation of self-avoiding semi-rigid chains [11]. The fractal dimension, which for bulk fractal clusters is evaluated by the $\ln I(q) = f(q)$ slope in the region of small q, is most pronounced for the CS·HCl·L-AscA sample. Quantitative indicators of the average radius of gyration of phase inhomogeneities of the supramolecular structure of the CS·HCl·L-AscA and CS·HCl·D-AscA plates also differ (Table 1). E.g., the CS·HCl·D-AscA sample is characterized by a larger average size of scattering domains and a wider range of R_n values.

The volume size distribution functions of scattering domains calculated from the SAXS curves for the CS·HCl·L-AscA (*a*) and CS·HCl·D-AscA plates show a bimodal character with two maxima. The average size R of the dominant fraction of domains (Fig. 3, first maximum) correlates with the average radius of gyration of scattering inhomogeneities (Table 1).

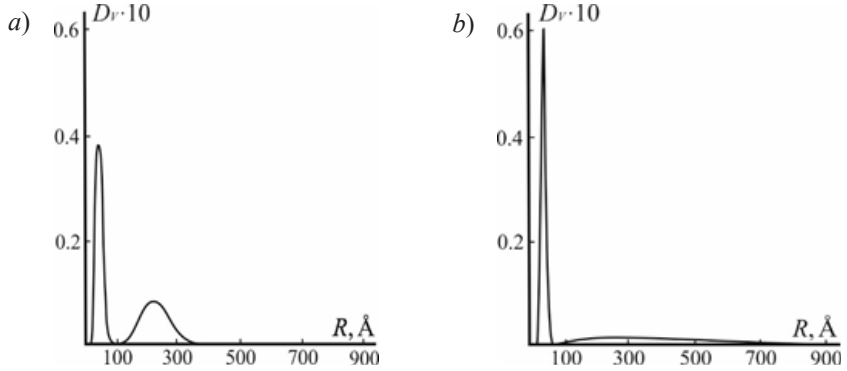

Fig. 3. Volume size distribution functions of scattering domains for our hydrogel plates based on CS·HCl·L-AscA (*a*) and CS·HCl·D-AscA (*b*)

The wider range of R_n is due to the fact that when calculating the average values of the radius of gyration, all scattering domains are taken into account, including the largest ones, whose weight fraction in the total supramolecular structure of the samples under study is relatively small (the second maximum). It is noteworthy that the amplitude of the $D_V(R)$ function, which is proportional to the electron density of scattering objects and, accordingly, the volume fraction of the main fraction of scattering domains, is much higher for CS·HCl·D-AscA. A narrower width of the distribution of the predominant fraction of scattering domains by R is also a distinctive feature of this sample.

Conclusion

Our comparative analysis of the structure of thin hydrogel plates of chitosan L- and D-ascorbate-hydrochloride carried out in this work by TEM and SAXS gives grounds to conclude that the materials differ in their supramolecular ordering and dimensional characteristics of phase inhomogeneities. The TEM images of plates made from CS·HCl·L-AscA reveal more branched

dendrite-like structures with a smaller branch width than those made from CS·HCl·D-AscA. The SAXS indicatrices show the fractal organization of nanosized inhomogeneities of the hydrogel spatial network with the largest average size of scattering objects for the CS·HCl·D-AscA sample. The volume size distribution functions of scattering domains have a bimodal character with the larger amplitude and the narrower distribution of the main fraction of nanostructures for CS·HCl·D-AscA.

The experiments performed, as well as our previous studies [12–14], indicate the important role of the (L-, D-) ascorbic acid isomer used to dissolve chitosan in the design of polymeric materials with a given spatial organization. Hydrogel plates made from CS·HCl·L-AscA and CS·HCl·D-AscA can be very promising in creating a sensitive layer of optical sensors for recognizing enantiomers of biologically active and medicinal compounds, separating racemic mixtures of optically active substances, detecting chiral molecules and even chiral nanoparticles and quantum dots.

REFERENCES

1. **Huang W. C., Chi H. S., Lee Y. C., Lo Y. C., Liu T. C., Chiang M. Y., Chen H. Y., Li S. J., Chen Y. Y., Chen S. Y.,** Gene-embedded nanostructural biotic–abiotic optoelectrode arrays applied for synchronous brain optogenetics and neural signal recording, ACS Appl. Mater. Interfaces. 11(12) (2019) 11270–11282.

2. **Wang X., Wolfbeis O. S.,** Fiber-optic chemical sensors and biosensors (2015–2019), Anal. Chem. 92(1) (2019) 397–430.

3. **Rehmat Z., Mohammed W. S., Sadiq M. B., Somarapalli M., Anal A. K.,** Ochratoxin A detection in coffee by competitive inhibition assay using chitosan-based surface plasmon resonance compact system, Colloids Surf. B. 174 (2019) 569–574.

4. **Boruah B. S., Biswas R.,** In-situ sensing of hazardous heavy metal ions through an ecofriendly scheme, Optics and Laser Technology. 137 (2021) 106813.

5. **Mironenko A. Yu., Sergeev A. A., Nazirov A. E., Modin E. B., Voznesenskiy S. S., Bratskaya S. Yu.,** H2S optical waveguide gas sensors based on chitosan/Au and chitosan/Ag nanocomposites, Sensors and Actuators B: Chemical. 225 (2016) 348–353.

6. **Jang J., Kang K., Raeis-Hosseini N., Ismukhanova A., Jeong H., Jung C., Kim B., Lee J.-Y., Park I., Rho J.,** Self-powered humidity sensor using chitosan-based plasmonic metal–hydrogel–metal filters, Adv. Opt. Mater. 8 (2020) 1901932.

7. **Mashile P. P., Nomngongo P. N.,** Magnetic cellulose-chitosan nanocomposite for simultaneous removal of emerging contaminants: adsorption kinetics and equilibrium studies, Gels. 7 (4) (2021) 190–210.

8. **Lin Y.-J., Chuang W.-T., Hsu, S.-H.,** Gelation mechanism and structural dynamics of chitosan self-healing hydrogels by in situ saxs and coherent x-ray scattering, ACS Macro Lett. 8 (11) (2019) 1449–1455.

9. **Postnova I., Silant'ev V., Sarin S., Shchipunov Yu.,** Chitosan hydrogels and bionanocomposites formed through the mineralization and regulated charging, Chem. Rec. 18 (7-8) (2018) 1247–1260.

10. **Ashrafi H., Azadi A.,** Chitosan-based hydrogel nanoparticle amazing behaviors during transmission electron microscopy, Inter. J. Biolog. Macromolec. 84 (2016) 31–34.

11. **Ventura I., Bianco-Peled H.,** Small-angle X-ray scattering study on pectin–chitosan mixed solutions and thermoreversible gels, Carbohydr. Polym. 123 (2015) 122–129.

12. **Shipovskaya A. B., Malinkina O. N., Gegel N. O., Zudina I. V., Lugovitskaya T. N.,** Structure and properties of chitosan salt complexes with ascorbic acid diastereomers, Russ. Chem. Bull. 70 (2021) 1765–1774.

13. **Shipovskaya A. B., Zhuravleva Yu. Yu., Khonina T. G., Malinkina O. N., Gegel N. O.,** Influence of the ascorbic acid isoform on the sol-gel synthesis kinetics and properties of silicon-chitosan-containing glycerohydrogel plates, J. Sol-Gel Sci. Technol. 92 (2) (2019) 349–358.

14. **Gegel N. O., Zhuravleva Yu. Yu., Shipovskaya A. B., Malinkina O. N., Zudina I. V.,** Influence of chitosan ascorbate chirality on the gelation kinetics and properties of silicon-chitosan-containing glycerohydrogels, Polymers. 10 (3) (2018) 259–275.

15. **Ogawa K., Nakata K., Yamamoto A., Nitta Y., Yui T.,** X-ray study of chitosan L-and D-ascorbates, Chem. Mater. 8 (9) (1996) 2349–2351.

16. **Larchenko E. Yu., Shadrina E. V., Khonina T. G., Chupakhin O. N.,** New hybrid chitosan–silicone containing glycerohydrogels, Mendeleev Commun. 4 (24) (2014) 201–202.

17. **Feigin L., Svergun D. I.,** Structure analysis by small angle X-ray and neutron scattering. Plenum Press, NewYork, 1987.

18. **Svergun D. I.,** Determination of the regularization parameter in indirect-transform methods using perceptual criteria, J. Appl. Cryst. 25 (1992) 495–503.

THE AUTHORS

SHIPOVSKAYA Anna B.
Shipovskayaab@yandex.ru
ORCID: 0000-0003-1916-4067

BABICHEVA Tatyana S.
tatyana.babicheva.1993@mail.ru
ORCID: 0000-0002-6655-8483

GEGEL Natalia O.
gegelno@yandex.ru
ORCID: 0000-0001-5724-7571

Received 15.07.2022. Approved after reviewing 05.08.2022. Accepted 05.08.2022.